Article

Current Biology

A RhoA Signaling Pathway Regulates Dendritic Golgi Outpost Formation

Graphical Abstract

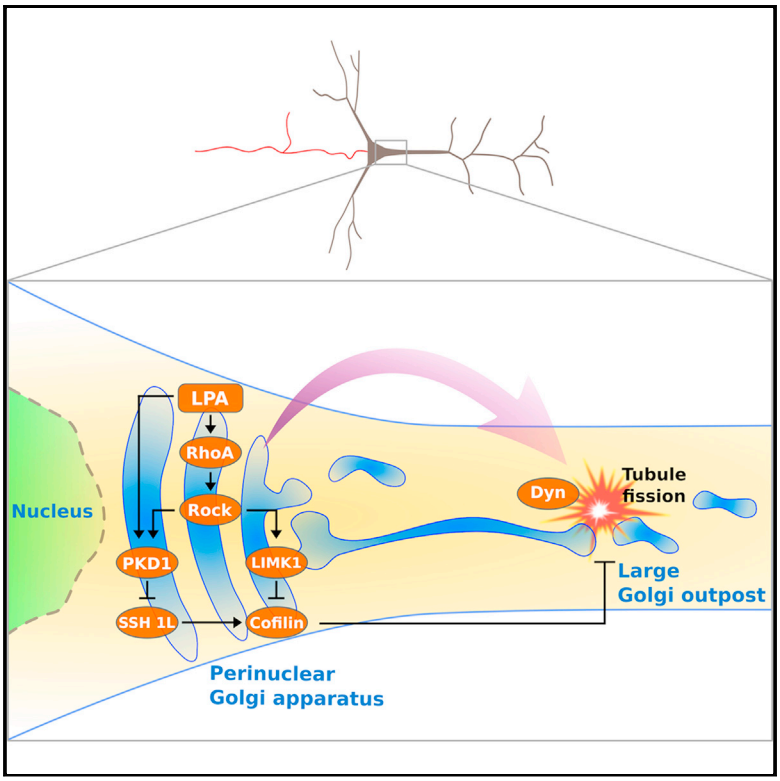

Authors

Gonzalo Quassollo, Jose Wojnacki, ..., Andrés Couve, Alfredo Cáceres

Correspondence

acaceres@immf.uncor.edu

In Brief

Dendritic Golgi outposts (GOPs) shape dendritic morphology and serve as platforms for the local delivery of synaptic receptors. Quassollo et al. show that GOPs destined to major dendrites are generated by deployment and fission of Golgi-apparatus-derived tubules. A RhoA signaling pathway regulates the fission event and GOP formation.

Highlights

- RhoA regulates biogenesis of Golgi outposts (GOPs) in major dendrites
- Deployment and fission of Golgi-apparatus-derived tubules generate GOPs
- LIMK1 and PKD1 control tubule fission by inactivating Slingshot and Cofilin
- RhoA and Rock activate LIMK1 and PKD1 at the Golgi, promoting GOP formation

Quassollo et al., 2015, Current Biology *25*, 971–982
April 20, 2015
http://dx.doi.org/10.1016/j.cub.2015.01.075

Current Biology
Article

A RhoA Signaling Pathway Regulates Dendritic Golgi Outpost Formation

Gonzalo Quassollo,[1,2,6] Jose Wojnacki,[1,2,6] Daniela A. Salas,[4] Laura Gastaldi,[1,2] María Paz Marzolo,[5] Cecilia Conde,[1,2,3] Mariano Bisbal,[1,2,3] Andrés Couve,[4] and Alfredo Cáceres[1,2,3,*]
[1]Laboratorio Neurobiología, INIMEC-CONICET, Av. Friuli 2434, 5016 Córdoba, Argentina
[2]Universidad Nacional de Córdoba, Av. Haya de la Torre s/n, 5000 Córdoba, Argentina
[3]Instituto Universitario Ciencias Biomédicas Córdoba, Av. Friuli 2786, 5016 Córdoba, Argentina
[4]Programa de Fisiología y Biofísica, Instituto de Ciencias Biomédicas, Biomedical Neuroscience Institute, Facultad de Medicina, Universidad de Chile, Independencia 1027, 8380453 Santiago, Chile
[5]Departamento de Biología Celular y Molecular, Facultad de Ciencias Biológicas, Pontificia Universidad Católica de Chile, Avda. Libertador Bernardo OHiggins 340, 8331010 Santiago, Chile
[6]Co-first author
*Correspondence: acaceres@immf.uncor.edu
http://dx.doi.org/10.1016/j.cub.2015.01.075

SUMMARY

The neuronal Golgi apparatus (GA) localizes to the perinuclear region and dendrites as tubulo-vesicular structures designated Golgi outposts (GOPs). Current evidence suggests that GOPs shape dendrite morphology and serve as platforms for the local delivery of synaptic receptors. However, the mechanisms underlying GOP formation remain a mystery. Using live-cell imaging and confocal microscopy in cultured hippocampal neurons, we now show that GOPs destined to major "apical" dendrites are generated from the somatic GA by a sequence of events involving: (1) generation of a GA-derived tubule; (2) tubule elongation and deployment into the dendrite; (3) tubule fission; and (4) transport and condensation of the fissioned tubule. A RhoA-Rock signaling pathway involving LIMK1, PKD1, slingshot, cofilin, and dynamin regulates polarized GOP formation by controlling the tubule fission. Our observations identify a mechanism underlying polarized GOP biogenesis and provide new insights regarding involvement of RhoA in dendritic development and polarization.

INTRODUCTION

The participation of dendritic Golgi outposts (GOPs) [1–5] in post-ER trafficking has been established by imaging the transport of GFP-VSV-G ts045 in cultured hippocampal neurons [3]. Interestingly, NMDA receptors are sorted from AMPA receptors at the ER, bypassing the somatic GA and merging instead with dendritic GOPs [6]. Thus, mini-GA may serve as secretory platforms for the local delivery of synaptic receptors, and therefore have a role in synaptic plasticity.

GOPs also contribute to dendritic growth and branch dynamics [7, 8], perhaps by regulating the amount of cargo being trafficked to each branch [4]. Accordingly, disruption of the dynein/dynactin adaptor Lava-lamp or dynein mutations in *Drosophila* sensory neurons reduces the number of GOPs and dendritic branches [7–9]. It was proposed that, in *Drosophila* dendritic arborization (da) neurons, GOPs shape dendritic morphology by functioning as sites of acentrosomal microtubule nucleation [10, 11]. However, another recent study has challenged these observations by showing that, in two different types of *Drosophila* neurons, γ-tubulin controls dendritic microtubule nucleation independently of GOPs [12].

Regardless, the crucial question of how GOPs are generated remains unanswered. One possibility is the local de novo production of GOPs from the ER as in the case of Golgi reassembly at the cell periphery in non-neuronal cells [13]. Alternatively, GOPs could be generated after somatic Golgi fragmentation, a phenomenon induced by increased neuronal activity [14], followed by dispersal of remnant membranes that serve as templates to rebuild satellite Golgi stacks. In the present study, we have evaluated whether or not GOPs can be generated from the central somatic GA and tested the role of components of the Golgi fission machinery, such as LIMK1 [15, 16] or Protein Kinase D1 (PKD1) [17, 18], and their upstream regulators and downstream effectors in such a process. Our observations identify a RhoA-Rho kinase (Rock) signaling pathway that regulates polarized GOP formation in developing neurons.

RESULTS

GOPs in Major Dendrites Are Generated from the Somatic GA

Previous immunofluorescence and electron microscope studies have shown that in mammalian neurons GOPs preferentially localize to a single dendrite, which corresponds to the apical dendrite of cortical pyramidal neurons in situ or to the major dendrite of cultured hippocampal neurons [3]; it was proposed that segregation of GOPs precedes and is required for the elaboration of polarized dendritic arbors [3].

To evaluate whether or not polarized GOPs could derive from the somatic GA in a first set of experiments, we analyzed their morphodynamics by live-cell imaging [15, 19]. To this end, 14 days in vitro (DIV) hippocampal pyramidal neurons were transfected with sialyl-transferase 2 (SialT2, a resident enzyme

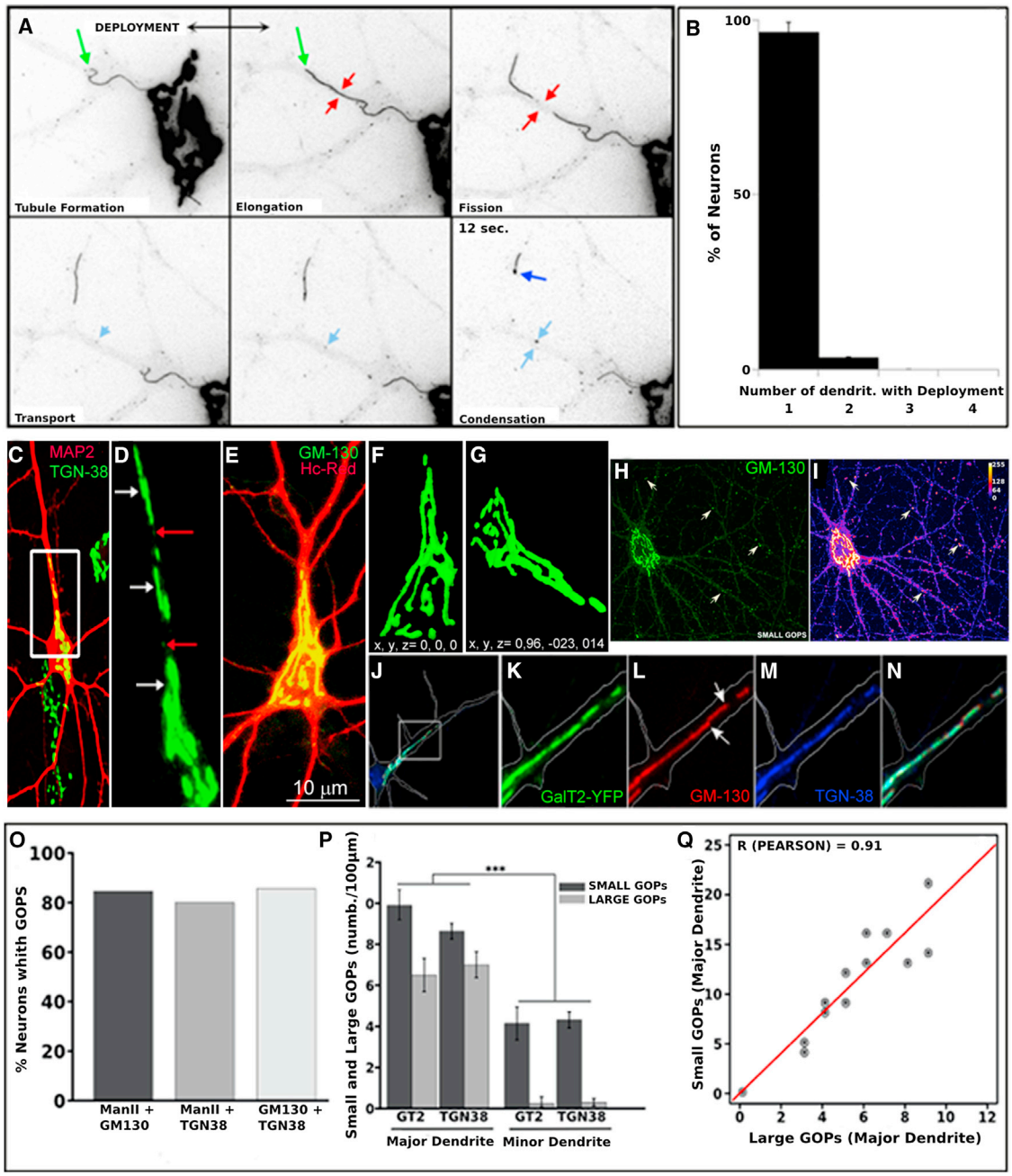

Figure 1. Generation of GOPs in Major Dendrites of Cultured Hippocampal Neurons

(A) A time-lapse sequence showing the generation of a large GOP from the somatic GA. Images were taken using a spinning disk confocal microscope and each of them represents maximal projections from at least three optical slices. The neuron expresses SialT2-YFP (black). Green arrows point to the tip of a GAdT; the red arrows to the region where the tubule undergoes fission; the dark-blue arrow to the region where the fissioned tubule begins to condense; the light-blue arrows to a small vesicle-like structure that appears at the site where the severing took place.

(B) Graphs showing percentage of neurons displaying Golgi deployment in one or more dendrites.

(C) Image showing the morphology of a 14 DIV hippocampal pyramidal neuron stained for MAP2 (red) and TGN-38 (green). Note that TGN-38 labeling is restricted to the cell body and the largest dendrite; TGN-38 also labels the GA of MAP2 negative cells.

(D) A high-magnification view of the insert shown in (C); the white arrows point to large GOPs, while the red ones to presumptive sites of fission/breakdown.

(E) An example of a 14 DIV hippocampal neuron, transfected with Hc-Red and stained for GM-130 (green).

(F and G) 3D reconstructions of the GA of the cell shown in (E); the corresponding rotation angles for the x, y, and z axes are indicated.

(H) Another example of a 14 DIV cultured neuron stained for GM-130, showing the distribution of the somatic GA and of large (proximal dendrites) and small GOPs (high-order dendritic branches, arrows).

(I) A pseudo color (Fire LUT) view of the image shown in (H).

(J) Merge image showing colocalization of GalT2-YFP (green), GM-130 (red), and TGN-38 (blue) in a long GAdT that enters a major dendrite.

(legend continued on next page)

of the *cis*-Golgi), or galactosyl-transferase 2 (GalT2, a resident transferase preferentially associated with the *trans*-Golgi), or β-1, 4-N-acetylgalactosaminyltransferase (GalNAcT, a resident transferase associated with the *trans*-Golgi) [15, 20–22] fused to yellow fluorescent protein (YFP) or m-Cherry and examined 16–18 hr post-transfection by spinning disk confocal microscopy. Live-cell image examination of neurons expressing ectopic glycosil-transferases revealed that the GA is a highly dynamic organelle with tubulo-vesicular structures emerging from the stacks and entering (deployment) into dendrites. A representative time-lapse sequence from a neuron expressing SialT2-YFP is displayed in Figure 1A. The images show a rapid sequence of events (~12 s) involving: (1) Golgi deployment [23] (Figure 1A, green arrows) into a dendrite; (2) tubule fission (Figure 1A, red arrows); (3) anterograde transport of the distal tubule; and (4) condensation/shrinkage of the distal tubule (Figure 1A, dark-blue arrow). In most cases, deployment occurs in a single process, usually the largest dendrite (Figure 1B). In a small percentage (less than 5%) of neurons, deployment was observed in two dendrites and was never detected in three or more dendrites (Figure 1B). The half-life of Golgi-derived tubules was approximately 20 s and the number of tubules generated per minute 2.5 ± 0.2, in agreement with values reported previously for younger neurons [15]. In addition, the live-cell imaging analysis revealed the presence of small vesicular structures in secondary or high-order dendritic branches that move in the anterograde and retrograde direction (Figure 1A). We failed to detect somatic GA fragmentation followed by dispersal and transport into dendrites; fragmentation was only observed in neurons expressing high levels of ectopic resident transferases.

The morphology and distribution of the somatic GA and GOPs was also analyzed by confocal microscopy in fixed cultures stained for endogenous Golgi proteins, such as mannosidase II or GM130 or TGN38, and expressing ectopic glycosil-transferases (Figures 1C–1N). Approximately 80% of 14 DIV cultured neurons display GOPs containing at least two endogenous Golgi markers (e.g., mannosidase 2 and TGN38 or GM130 and TGN38; Figures 1J–1O) with most of them localizing to major dendrites and presumably associated with tubule deployment and fission.

Two types of GOPs were identified: (1) large GOPs (>1.0 μm in size) that preferentially localized to first- or second-order segments of major dendrites (Figures 1C–1G and 1J–1N); and (2) small GOPs (0.3–1.0 μm size) present in first-order segments of minor dendrites, as well as second- or higher-order segments of all types of dendrites (Figures 1H and 1I, arrows). They account for more than 95% of GOPs in minor dendrites. The density of small GOPs (number per 100 μm) was higher in the main dendrite than in the minor ones of a given neuron (Figure 1P). Besides, in the main dendrite a high correlation was observed between the number of small GOPs in high-order dendritic branches and the presence of large GOPs in first- or second-order segments of the main dendrite (Figure 1Q). Our analysis also showed that more than 90% of large GOPs observed after ectopic expression of glycosil-transferases contain endogenous Golgi markers that colocalize with the transfected proteins (Figures 1J–1N). Together, these observations suggest that deployment of somatic Golgi-derived tubules (GAdTs) or stacks followed by fission and transport may account for the generation of GOPs in the major dendrite of cultured hippocampal neurons.

LIMK1 and PKD1 Promote GOP Formation in Major Dendrites

To test whether or not fission is a key step for GOP generation, we decided to examine the role of components of the Golgi-fission machinery [18, 24]. One of such elements is LIMK1 [15, 25], a serine threonine kinase that phosphorylates and inactivates cofilin, an actin dynamizing factor [25–27]. LIMK1 is enriched in brain tissue where it regulates axon-dendrite development [15, 28], spine formation [29], and synaptic plasticity [29]. In both neuronal and non-neuronal cells, LIMK1 localizes to the GA where it regulates trafficking of post-Golgi vesicles in a cofilin-dependent manner [15, 16]. Most of the neurons expressing a kinase dead (kd) variant [15, 16] of LIMK1 displayed a somatic GA with either elongated stacks or tubules entering major dendrites (Figures 2A–2C); quantitative analysis revealed a 2- to 3-fold increase in the number of cells displaying Golgi deployment without fission (Figure 2D). This was accompanied by a significant reduction in the number of both large and small GOPs in the main dendrite (Figures 2E and 2F). Live image analysis revealed that neurons expressing LIMK1-kd display GAdTs, which last for more than a minute and show no signs of fission (data not shown; see also below). Suppression of LIMK1 with a specific small hairpin RNA (shRNA) (Figures 2G–2K; see also Supplemental Experimental Procedures) also reduced the number of large and small GOPs, with neurons displaying long tubules with few sites of fragmentation (Figures 2D–2F, 2L, and 2M). Interestingly, after LIMK1 inactivation or suppression, the number of large and small GOPs decreased only in the major dendrite, where small GOPs fell to values similar to those found in minor dendrites. Ectopic expression of LIMK1-wt had the opposite effect, increasing the number of neurons displaying fragmented GAdTs (Figure 2D), as well as the number of large and small GOPs in the major dendrite (Figures 2E, 2F, and 2N–2P). Live image analysis also revealed increased fission of GAdTs in neurons expressing LIMK1-wt (Figure S1); the average number of fission events was more than two times higher in neurons expressing LIMK1-wt than in control cells (mock-transfected or non-transfected).

In the next series of experiments, we tested the role of PKD1 in GOP formation. PKD1 is a diacylglycerol (DAG)-binding Ser/Thr kinase, implicated in the regulation of plasma membrane

(K–M) High-magnification views of the insert shown in (J); note that there are regions of the deployed tubule where the GM-130 signal predominates over the two other markers (arrows in L).

(N) Merge image of the insert shown in (J).

(O) Graph showing percentage of dendritic GOPs expressing different Golgi markers.

(P) Graphs showing the number of large and small GOPs in major and minor dendrites as revealed by expression of GalT2-YFP (GT2) or staining with TGN38. Note the absence of large GOPs in minor dendrites and that the number of small GOPs is higher in major dendrites than in the minor ones.

(Q) Graph showing that there is high and significant correlation between the number of large and small GOPs in major dendrites.

Error bars in each of the graphs represent the SEM.

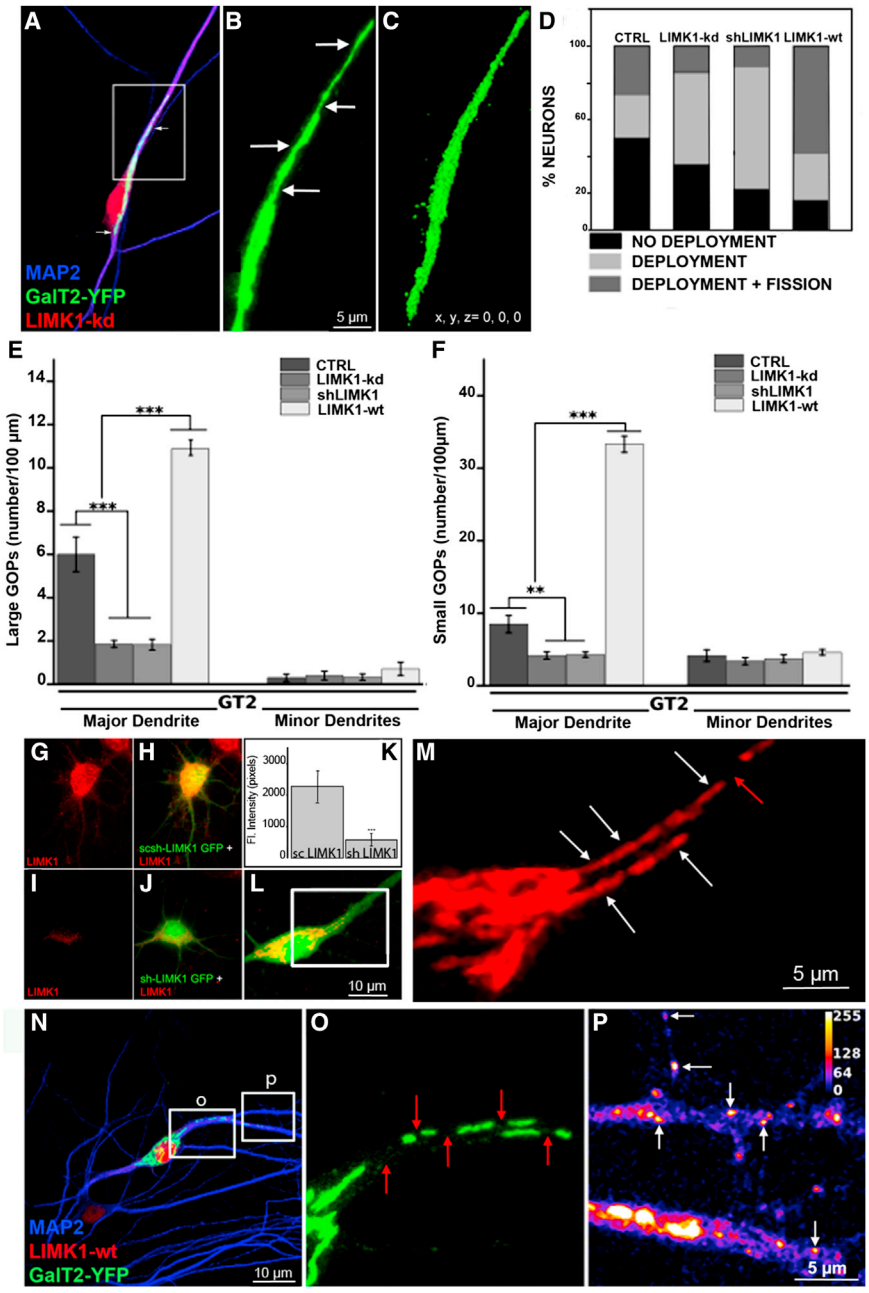

Figure 2. LIMK1 Regulates GOP Formation in Major Dendrites

(A) Image showing the morphology of the GA in a 14 DIV hippocampal pyramidal neuron expressing LIMK1-kd. Note that a long GAdT enters a single dendrite.

(B) A high-magnification view of the insert shown in (A); no signs of fission are observed along the deployed tubule (white arrows).

(C) A 3D reconstruction of a region of the GA from the cell shown in (A) (arrows).

(D) Graphs showing percentages of neurons displaying no GA deployment, GA deployment without fission, and GA deployment with fission after expression of LIMK1-kd, or sh-LIMK1, or LIMK1-wt.

(E and F) Graphs showing changes in the number of large (E) and small (F) GOPs in neurons expressing LIMK1-kd, or sh-LIMK1, or LIMK1-wt.

(G–J) Images showing LIMK1 immunofluorescence (red) in a neuron expressing a scrambled sh-LIMK1-GFP plasmid (control group, G and H) and in another one expressing the sh-LIMK1-GFP plasmid (I and J).

(K) Graph showing that the sh-LIMK1 significantly reduces LIMK1 immunofluorescence.

(L) Image showing the morphology of the GA after expression of sh-LIMK1-GFP (green) in a neuron co-expressing GalT2-Cherry.

(M) High-magnification view of the insert shown in (L); note the presence of two long GAdTs (white arrows) with a single site of fission/breakdown (red arrow).

(N) Image showing the morphology of the GA in a neuron expressing LIMK1-wt (red), GalT2-YFP, and stained for MAP2 (blue).

(O) High-magnification view of one of the inserts (o) shown in (N). Note the presence of several large GOPs; the red arrows point to presumptive sites of fission/breakdown.

(P) A pseudo color (Fire LUT) high-magnification view of the insert (p) shown in (N). Note the presence of numerous large and small (arrows) GOPs. Bars in (A), (G)–(J), and (L), 10 μm, and in (B) and (O), 5 μm. Error bars in each of the graphs represent the SEM.

directed transport [30]. Suppression and/or inactivation of PKD1 halt a fission pathway involved in the exit and sorting of carriers containing either basolateral [31] or dendritic [17] membrane proteins, such as the transferrin receptor.

Expression of PKD1-kd [17, 31] selectively inhibited GOP formation in major dendrites. Thus, major dendrites of transfected neurons displayed long GAdTs and a concomitant reduction in the number of large and small GOPs (Figures 3A–3H). A similar phenotype was observed after targeting PKD1 with a specific shRNA [17] (Figures 3F–3J). By contrast, upregulation of PKD1 by ectopic expression of a constitutive active (CA) variant increased the number of large and small GOPs in major dendrites (Figures 3F–3H, 3K, and 3L).

None of the above-described treatments significantly altered the position or morphology of the central GA. Parameters such as perimeter, circularity, roundness, and aspect ratio (see Supplemental Experimental Procedures) were unaltered after expression of PKD-CA, PKD1-kd, LIMK1-wt, or LIMK1-kd (Figure S2). Also, none of them altered the distribution or density of dendritic microtubules, as revealed by staining for MAP2 or acetylated α-tubulin (data not shown).

LIMK1 and PKD1-Mediated GOP Formation Involves Cofilin Inactivation and Is Dynamin Dependent

Suppression of the actin-dynamizing factors (ADF/cofilin) inhibits export of soluble secretory and integral membrane proteins from the TGN [16, 32–34]. Since ectopic expression of LIMK1 induces phosphorylation of cofilin at the GA [15] and

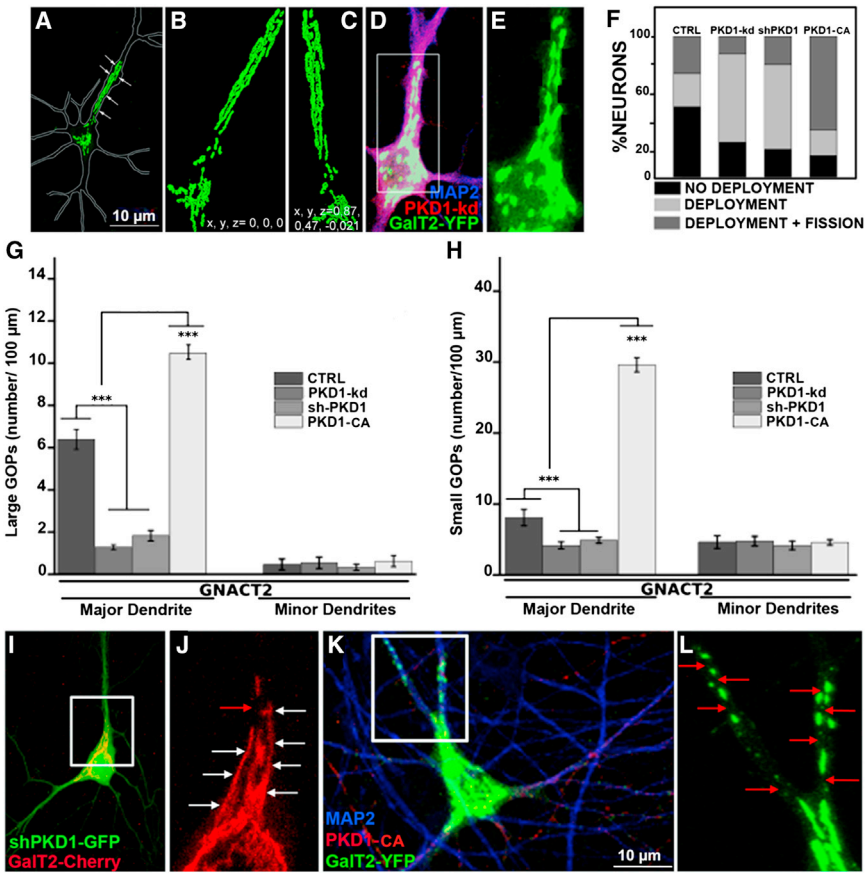

Figure 3. PKD1 Regulates GOP Formation in Major Dendrites

(A) Image showing the morphology of the GA in a 14 DIV hippocampal pyramidal neuron expressing PKD1-kd (not shown) and stained for TGN-38 (green). Note that long GAdTs enter the major dendrite (arrows).

(B and C) 3D reconstructions of the GA of the neuron shown in (A).

(D) Merged image showing the morphology of another neuron transfected with PKD1-kd (red) plus GalT2-YFP (green) and stained for MAP2 (blue).

(E) A high-magnification view of the insert shown in (D).

(F) Graphs showing percentages of neurons displaying no GA deployment, GA deployment without fission, and GA deployment with fission after expression of PKD1-kd, or sh-PKD1, or PKD1-CA.

(G and H) Graphs showing changes in the number of large (G) and small (H) GOPs in neurons expressing PKD1-kd, or sh-PKD1, or PKD1-CA.

(I) Image showing the morphology of the GA after expression of sh-PKD1-GFP (green) in a neuron co-expressing GalT2-Cherry (red).

(J) High-magnification view of the insert shown in (I). Note the presence of several long GAdTs (white arrows) with only one site of fission/breakdown (red arrow).

(K) Image showing the morphology of the GA in a neuron expressing PKD1-CA (red), GalT2-YFP (green), and stained for MAP2 (blue).

(L) High-magnification view of the insert shown in (K). Note the presence of many GOPs; the red arrows point to presumptive sites of fission/breakdown.

Bars in (A) and (I), 10 μm, and in (D) and (K), 10 μm. Error bars in each of the graphs represent the SEM.

LIMK1-promoted p75 trafficking is dependent on cofilin inactivation [16], we evaluated the role of cofilin in GOP formation and whether or not it acts downstream of LIMK1. To this end, we first tested the effect of S3A-cofilin, a CA variant [15, 16]. Ectopic expression of this mutant increased the number of neurons displaying GAdTs without signs of fragmentation and decreased number of large and small GOPs in the major dendrite (Figures 4A, 4B, 4F, and 4G); these observations are consistent with a previous study where we showed by live imaging that 7 DIV hippocampal neurons expressing S3A-cofilin extend long GAdTs that last for almost 2 min without undergoing fission (see Figure 4 in [15]). By contrast, expression of S3E-cofilin, a constitutive inactive mutant [27], had the opposite effect (Figures 4C–4G). Co-expression of S3A-cofilin significantly reduced the stimulatory effect of LIMK1-wt in GOP formation (Figures 4H, 4I, 4L, and 4M), while S3E-cofilin reduced the inhibitory effect of LIMK1-kd (Figures 4J–4M). Interestingly, S3E cofilin also stimulated GOP formation in neurons co-expressing PKD1-kd (Figures 5A–5C and 5H), while S3A cofilin reduced the stimulatory effect of PKD1-CA (Figures 5D, 5E, and 5H).

To further explore the mechanisms underlying fission and GOP formation, we tested the involvement of slingshot1 (SSH1) that belongs to a family of phosphatases that reactivate phosphorylated cofilin (P-cofilin) by dephosphorylation [35]. It was recently demonstrated that PKD-mediated phosphorylation at Ser 402 in SSH1 inhibits substrate binding and thus phosphatase activity, resulting in enrichment of P-cofilin [36]. We used wild-type SSH1 and SSH1-402 L, a mutant form of SSH1 that is not phosphorylated by PKD1 [36]. SSH1 (data not shown) or SSH1-402L reduced basal (Figures 5F and 5H) and PKD1-CA-stimulated GOP formation (Figures 5G and 5H). Together, these results suggest that both LIMK1 and PKD1 most likely control GOP formation by an actin-dependent mechanism involving cofilin.

Therefore, since dynamin 2 has been involved in the cofilin/actin-mediated exit of apical carriers in MDCK cells [16], it became of interest to evaluate its participation in GOP formation. A dn variant of dynamin 2 induced deployment of long and almost continuous GAdTs into the apical dendrite (Figures 5I, 5J, and 5M) and completely prevented LIMK1-wt- or PKD1-CA-stimulated GOP formation (Figures 5K–5M).

LPA Stimulates GOP Formation by Activating RhoA and PKD1 at the GA

In the final series of experiments, we sought to identify factors upstream of LIMK1 or PKD1 that might regulate GOP formation. Lysophosphatidic acid (LPA) is a phospholipid derivative abundant in the nervous system where it influences multiple events [37, 38]. Because LPA stimulates RhoA activity, an upstream regulator of LIMK1 [39], we evaluated its involvement in GOP

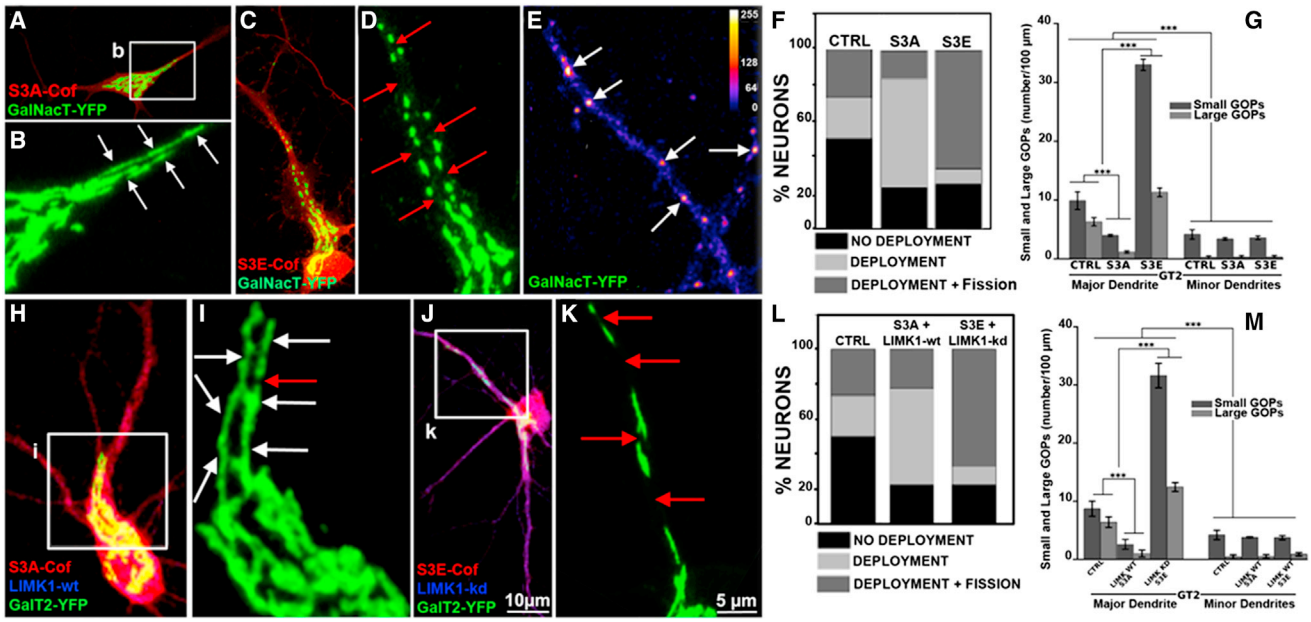

Figure 4. Cofilin Regulates GOP Formation in Major Dendrites

(A) Image showing the morphology of the GA in a 14 DIV hippocampal pyramidal neuron transfected with S3A-cofilin (red) and GalNacT-YFP (green).

(B) High-magnification view of the insert shown in (A). Note that two long GAdTs (white arrows) enter the major dendrite and have no sites of fission/breakdown.

(C) Image showing the morphology of the GA in a neuron transfected with S3E-cofilin (red) and GalNacT-YFP (green).

(D) A high-magnification view of the dendrite shown in (C); red arrows point to presumptive sites of fission.

(E) A pseudo color image (Fire LUT) from a S3E-transfected neuron showing numerous small GOPs (arrows) in high-order dendritic branches from a main dendrite.

(F) Graphs showing percentages of neurons displaying no GA deployment, GA deployment without fission, and GA deployment with fission in CTRL cells, or after expression of S3A, or S3E cofilin.

(G) Graphs showing changes in the number of large and small GOPs in CTRL neurons and in cells expressing S3A or S3E cofilin.

(H) Image showing the morphology of the GA from a neuron co-transfected with S3A cofilin (red), LIMK1-wt (blue, not displayed), and GalT2-YFP (green).

(I) High-magnification view of the insert shown in (H) as revealed by GalT2-YFP fluorescence. Note that two long GAdTs (white arrows) enter the major dendrite and only display one site of fission/breakdown (red arrow).

(J) Image showing the morphology of the GA from a neuron cotransfected with S3E cofilin (red), LIMK1-kd (blue), and GalT2-YFP (green).

(K) High-magnification view of the insert shown in (J). Note the presence of several large GOPs separated by presumptive sites of fission (red arrows).

(L) Graphs showing percentages of neurons displaying no GA deployment, GA deployment without fission, and GA deployment with fission in CTRL cells or after expression of S3A cofilin + LIMK1-wt or S3E cofilin + LIMK1-kd.

(M) Graphs showing changes in the number of large and small GOPs in CTRL neurons and in cells expressing S3A + LIMK1-wt or S3E cofilin + LIMK1-kd.

Bars in (B), (D), (E), (H), and (K), 5 μm, and in (C) and (J), 10 μm. Error bars in each of the graphs represent the SEM.

formation. To this end, 14 DIV hippocampal neurons were treated with increasing doses of LPA for different time periods and the number of GOPs evaluated in neurons expressing GalT2-YFP or in non-transfected cells stained for TGN38 and/or GM130. LPA (10 μM) induced a rapid (30 min) and significant increase in the number of GOPs, as well as in the percentage of neurons displaying them (Figures 6A–6E). This effect occurred preferentially in the major dendrite and was paralleled by an increase in phospho cofilin immunofluorescence in the Golgi area including the inner segment of the major dendrite (Figures 6F, 6G, and 6J). Additionally, both the effect on GOP formation and cofilin phosphorylation were blocked by treatment with the Rock inhibitor Y27632 (Figures 6H–6K, 6M, and 6N) and absent in neurons expressing LIMK1-kd (Figures 6L and 6N).

We then evaluated whether LPA could induce RhoA activation at the Golgi region. For such a purpose, we used a unimolecular fluorescence resonance energy transfer (FRET)-based biosensor [40, 41]. LPA (10 μM) induced a rapid (30 min) activation of RhoA in the region of primary dendrites containing large GOPs (Figures 7A–7G); thus, a high RhoA-FRET signal was detected in GOPs that stained positive for either GM130 or TGN38 in the major dendrite (Figures 7E and 7F; see also Figure S3). The GA localized in the neuronal soma showed a mild increase of RhoA activity compared to control neurons. Quantification of total RhoA activity of LPA-treated neurons versus control neurons showed a statistical significant increase (Figure 7G); however, no increase in RhoA activity was detected in minor dendrites.

Since a RhoA-Rock signaling pathway also activates PKD1 in migrating epithelial cells [42, 43], it became of interest to determine whether LPA-stimulated GOP formation also involves activation of PKD. For such a purpose, we used a recently developed fluorescent reporter for PKD activity [44]; this probe, designated as G-PKDrep-live, allows measurements of PKD activity at the TGN in live and fixed cells. Importantly LPA significantly increased the G-PKDrep-live signal in the region of the GA and GOPs (Figures 7H–7K and 7N) that stained positive for TGN38 within the major dendrite; accordingly, Y27632 attenuates

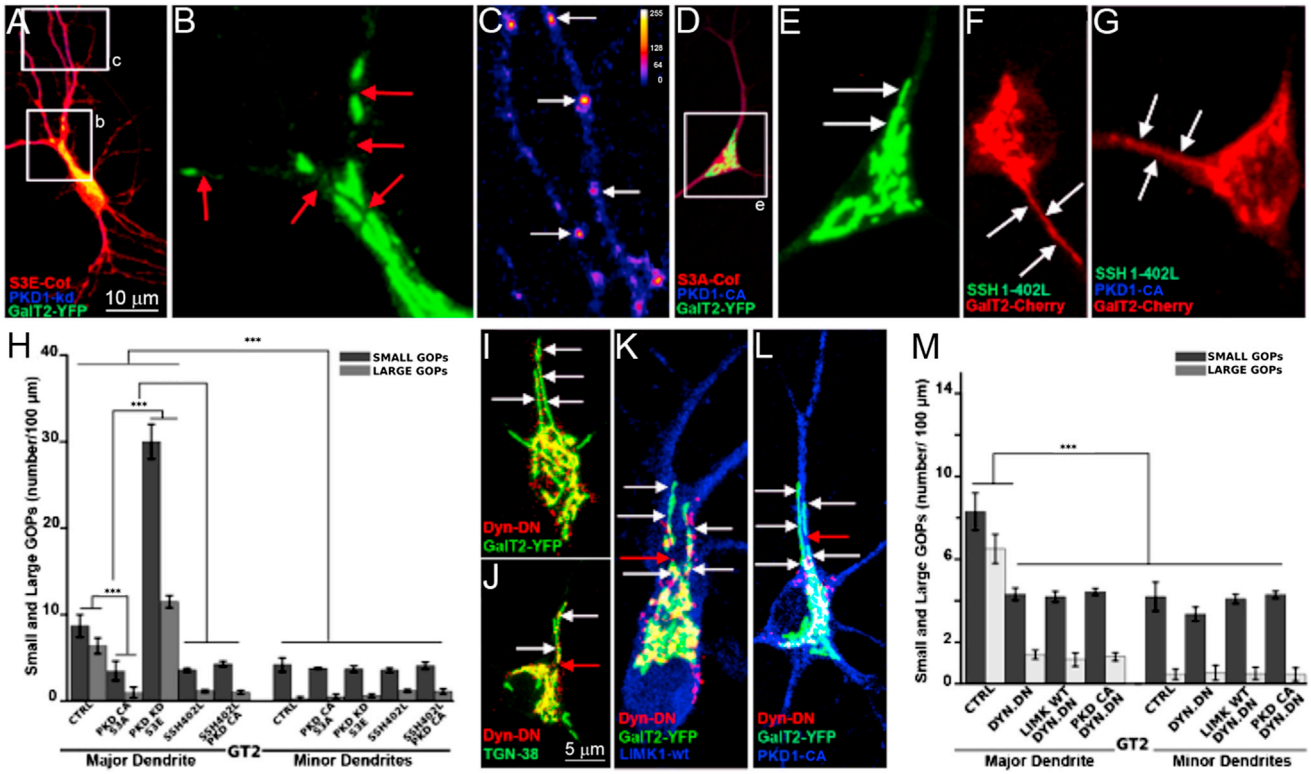

Figure 5. PKD1 Regulates GOP Formation Upstream of Cofilin and SSH1

(A) Image showing the morphology of the GA in a 14 DIV hippocampal pyramidal neuron co-expressing S3E cofilin (red), PKD1-kd (blue, not displayed), and GalT2-YFP (green).

(B) High-magnification view of the insert (b) shown in (A); the red arrows point to presumptive sites of fission.

(C) A high-magnification pseudo color (Fire LUT) image of the insert (c) shown in (A). Note the presence of small GOPs (white arrows) in high-order dendritic branches of the main dendrite.

(D) Image showing the morphology of the GA in a neuron co-expressing S3A-cofilin (red), PKD1-CA (blue, not displayed), and GalT2-YFP (green).

(E) High-magnification view of the insert (e) shown in (D).

(F) Image showing the morphology of the GA in a neuron transfected with SSH1-402L (green, not displayed) and GalT2-Cherry (red). Note that the GAdT (arrows) has no signs of fission/breakdown.

(G) A similar image but from a neuron co-transfected with SSH1-402L (green, not displayed) plus PKD1-CA (blue, not displayed) and GalT2-Cherry (red).

(H) Graphs showing changes in the number of large and small GOPs in CTRL neurons and in cells expressing PKD-CA plus S3A-cofilin, or PKD1-kd plus S3E cofilin, or SSH402L, or PKD1-CA plus SSH402L.

(I) Image showing the morphology of the GA in a neuron transfected with dynamin 2-dn (Dyn-DN, red) plus GalT2-YFP (green). Note that the GA displays several long tubules (white arrows) that show no signs of fission/breakdown.

(J) A similar image, but in this case the GA was visualized by staining for TGN-38 (green).

(K) Image showing the morphology of the GA in a neuron co-transfected with Dyn-DN (red), GalT2-YFP (green), and LIMK1-wt (blue). Note that the GA displays several long tubules (white arrows) with only one site of fission/breakdown (red arrow).

(L) A similar image but from a neuron co-transfected with PKD1-CA (blue, not displayed).

(M) Graphs showing changes in the number of large and small GOPs in control (CTRL) neurons and in cells expressing Dyn-DN, or Dyn-DN plus LIMK1-wt, or Dyn-DN plus PKD1-CA.

Bars in (A) and (D), 10 μm, and in (B), (C), (E)–(G), and (I)–(L), 5 μm. Error bars in each of the graphs represent the SEM.

LPA-induced PKD activation (Figures 7L–7N). Finally, we compared the time course of activation of RhoA and PKD using the corresponding biosensors. The results obtained showed that RhoA activation in the Golgi area occurs as early as 5 min after LPA (10 μM) remaining high for at least 30 min, while PKD activity starts to increase after RhoA activation (Figure 7O).

DISCUSSION

It has become increasingly evident that GOPs play major roles in regulating dendritic architecture and function [2, 3, 9, 45]. The presence of ER exit sites (ERESs) and ER Golgi intermediate compartment (ERGIC) sites/elements [4, 5, 46] in dendrites raise the possibility that GOPs may generate de novo by ER exocytosis at remote sites from the cell body. Alternatively, dendritic GOP biogenesis may be explained by fragmentation of the somatic GA followed by dispersion and minus-end microtubule-based transport into dendrites [8, 9, 45]. In both scenarios, dendrite-specific factors are likely to be required since stacked Golgi elements and/or GOPs have not been visualized in axons despite detection of ERES-ERGIC markers [47–49].

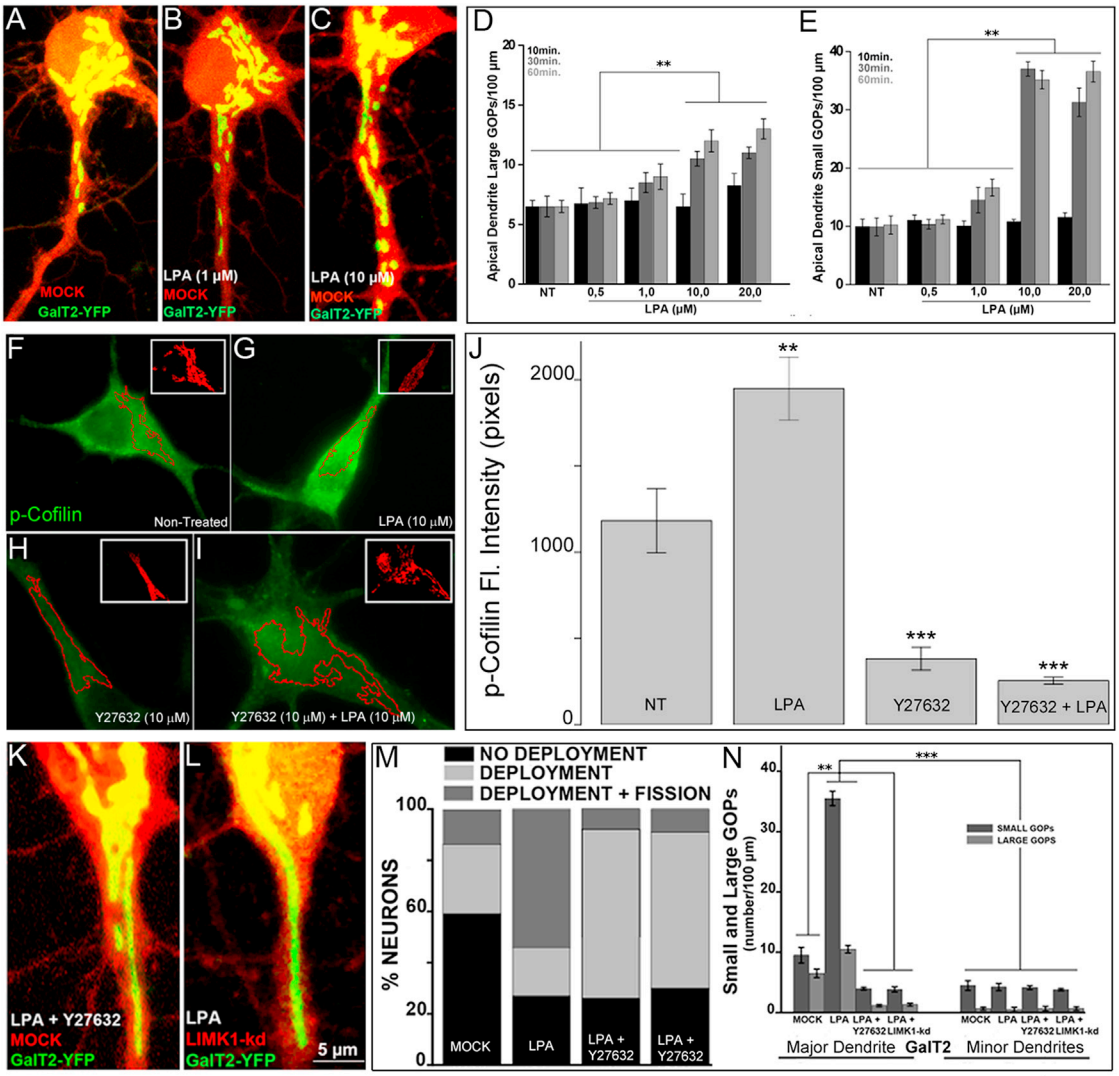

Figure 6. LPA Promotes GOP Formation in Major Dendrites

(A–C) Images showing the morphology of the GA in neurons transfected with mock vector plus GalT2-YFP and treated for 30 min with vehicle (DMSO, A), or LPA (1 μM, B), or LPA (10 μM, C).

(D and E) Graphs showing changes in the number of large (D) and small (E) GOPs in major dendrites of cultured hippocampal neurons treated for different periods of time with increasing doses of LPA. Control cells (NT) were treated with DMSO (vehicle) alone. Values significantly different (**$p < 0.01$) from NT.

(F–I) Images showing p-cofilin immunofluorescence (green) in NT and in neurons treated with LPA (10 μM for 30 min) or with Y27632 (10 μM) or Y27632 (10 μM) plus LPA (10 μM). In each image, the area corresponding to the GA as revealed by GM-130 immunolabeling (inserts, red) has been delineated; note that LPA increases p-cofilin immunofluorescence and that this effect is reduced by treatment with Y27632.

(J) Graphs showing measurements of p-cofilin immunofluorescence in NT and in cells treated with LPA (10 μM), or Y27632 (10 μM), or Y27632 + LPA. Values are expressed in pixels: 12 bits images (4,096 colors) were used for this quantification.

(K and L) Images showing the morphology of the GA in neurons form a culture treated for 30 min with LPA (10 μM) + Y27632 (K) or co-transfected with LIMK1-kd (L). The GA was visualized after expression of GalT2-YFP (green).

(M) Graphs showing percentages of neurons displaying no GA deployment, GA deployment without fission, and GA deployment with fission in CTRL neurons and in cells treated with LPA, or LPA plus Y27632, or LPA plus ectopic expression of LIMK1-kd.

(N) Graphs showing changes in the number of large and small GOPs in CTRL neurons and in cells treated with LPA or LPA plus Y27632 or LPA plus ectopic expression of LIMK1-kd. In all cases, LPA was used at a concentration of 10 μM for a 30-min period.

Error bars in each of the graphs represent the SEM.

In this study, we have identified a novel mechanism responsible for the polarized generation of GOPs, involving GAdTs. Tubules have been identified at the ERGIC [50], lateral rims of Golgi stacks, and the TGN where they form extensive networks involved in ER to *cis*-Golgi, intracisternal, and post-Golgi traffic events, respectively [51]. Tubules are also common features of the neuronal GA, being highly dynamic elements capable of extending several microns into the largest dendrite and having a

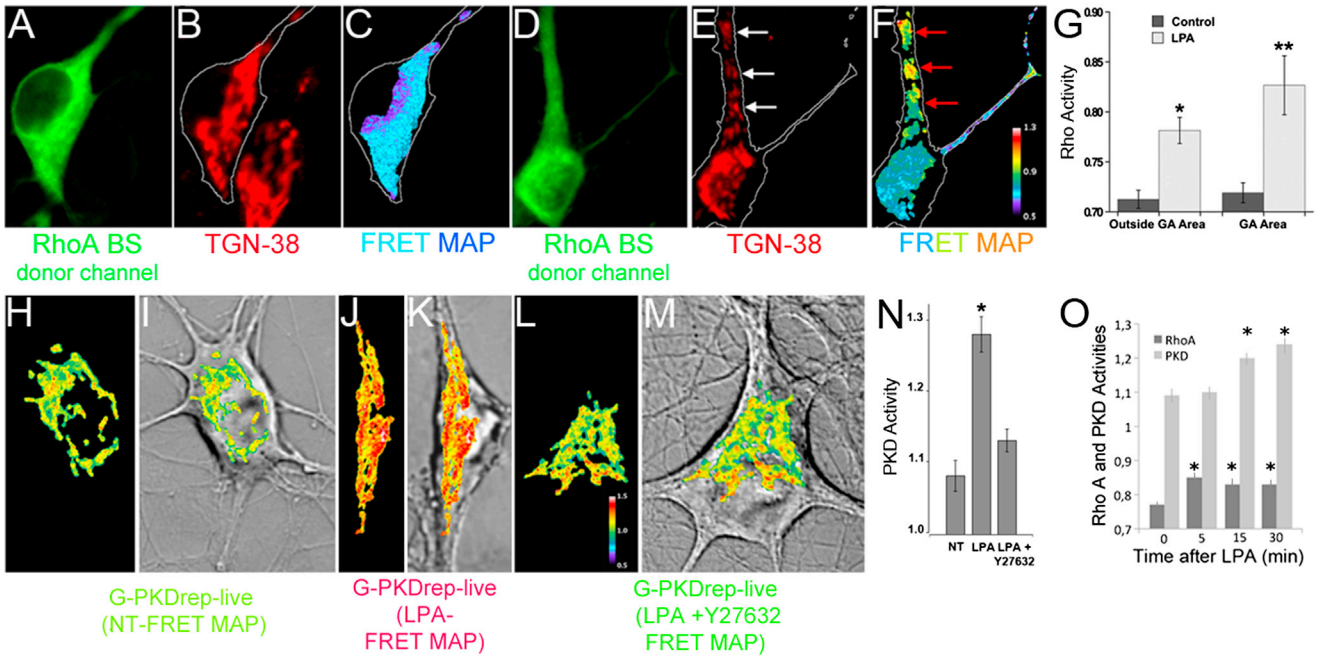

Figure 7. LPA Promotes Golgi-Associated RhoA and PKD1 Activities, as Revealed by FRET

(A and D) Fluorescent images from the donor emission channel (CFP excitation and emission) showing that the RhoA biosensor (BS) distributes throughout the cell in both DMSO- (A) and LPA- (D) treated neurons.

(B and E) Images showing the morphology of the GA of the cells shown in (A) and (D), respectively, as revealed by staining with TGN38 and Alexa 633 shown in red; note the presence of numerous GOPs (arrows) in the LPA-treated neuron (E).

(C and F) FRET map images showing active RhoA in the neurons displayed in (A) and (D), respectively. FRET maps (C and F) displaying RhoA activity associated with the GA (including GOPs) visualized by GM130 immunofluorescence (see also Figure S3); note that large GOPs (white arrows in E) display high RhoA activity (red arrows in F).

(G) Graphs showing RhoA activity (FRET signal) within and outside the GA in control and LPA-treated neurons.

(H, J, and L) Images showing FRET maps of non-treated (NT, H), LPA-treated (J), and LPA plus Y27632-treated (L) neurons transfected with the G-PKDrep-live biosensor.

(I, K, and M) FRET maps were superimposed on DIC images to show the morphology of the transfected neurons.

(N) Quantification of PKD activity, as defined by relative FRET efficiency (FRET channel over donor channel images), showing that Rock mediates LPA-dependent activation of the GA-PKD.

(O) Graphs showing time course of RhoA and PKD1 activations, as revealed by FRET, in the Golgi area of neurons treated with LPA. Note that RhoA activity increases before PKD1 activation. Significance: $^{**}p < 0.01$.

Error bars in each of the graphs represent the SEM.

half-life of approximately 20 s ([15]; this study). The mechanisms involved in their formation, as well as their molecular structure and composition, are only just beginning to be understood [51].

Our results suggest that GAdTs constitute a source for large GOPs in major dendrites. In agreement with this, live imaging of neurons expressing ectopic resident GA enzymes revealed that large GOPs are generated by a sequence of events involving extension and deployment of somatic GAdTs into a single dendrite followed by transport, fission, and condensation of the deployed tubule. Moreover, confocal microscopy of fixed neurons stained for endogenous GA markers and transfected with ectopic resident GA enzymes provides supporting evidence for the bona fide Golgi composition of these structures during the different stages.

As a matter of fact, one important aspect regarding GOP organization and function is whether or not they represent a complete, albeit smaller, version of the somatic GA with functionally polarized compartments and associated TGN. Our results show that GAdTs entering the major dendrite contain components of proximal and distal GA, as well as markers of the TGN, in agreement with a recent study showing multicompartment GOPs in dendrites of *Drosophila* neurons [11]; interestingly, some of them, like GalT2 or GM130 display partial colocalization within deployed tubules suggesting sub-organelle distribution resembling the somatic GA [51].

Tubule formation and deployment into dendrites are not sufficient to generate large GOPs. Fission of GA-deployed tubules is a crucial step for the polarized generation of large GOPs. In fact, up- or downregulation of tubule fission highly correlates with increased or decreased number of large GOPs. Accordingly, suppression of fission events dramatically reduces the number of large GOPs, whereas stimulation of fission has the opposite effect. It is likely that fission of large GOPs is also a mechanism for generating small GOPs in secondary and high-order branches of the main dendrite. Thus, we detected a high and significant correlation between the number of large and small GOPs in the main dendrite, not only in control condition, but also after up- or downregulation of fission/fragmentation of GAdTs.

Our study also newly identifies key components of the fission machinery that positively and negatively regulate the polarized generation of large and small GOPs, as well as upstream regulators and downstream effectors. In this context the results presented here reveal an important new function of LIMK1 and PKD1 in neuronal trafficking by mediating the fission of GAdTs required for polarized GOP formation. Several lines of evidence support this notion: First, suppression or inactivation of LIMK1 or PKD1 restrain GOP formation increasing the number of neurons displaying a major dendrite with long GAdTs with few or no signs of fragmentation. Second, overexpression of LIMK1-wt or PKD1 CA has the opposite effect, with neurons displaying major dendrites with significantly higher number of large and small GOPs and GAdTs showing extensive fragmentation, suggestive of enhanced fission. Third, these observations are in line with previous studies showing that both proteins are involved in fission events associated with the GA and specifically exit from the TGN of tubulo-vesicular carriers containing membrane proteins [16–18]. Besides, both types of LIMK1- and PKD1-mediated fission events (e.g., polarized GOP formation and exit of post GA carriers) involve downregulation of cofilin activity and are dynamin dependent. The fact that the single suppression of each of the kinases is sufficient to inhibit formation of large and small GOPs in the main dendrite suggests that LIMK1 and PKD1 act cooperatively on the final effector pathway, namely, cofilin-dynamin, rather than in a complementary or redundant manner. This might imply that a strong inhibition of cofilin activity is required for severing GAdTs. It may also represent an important difference with respect to other fission events involving reduction of cofilin activity. For example, in MDCK cells, fission and exit from the TGN of p75-containing apical carriers is sensitive to the single suppression of LIMK1 [16], but not of PKD1; conversely, downregulation of PKD1 halts exit of basolateral or dendritic carriers but does not affect apical or axonal ones [17, 18]. Perhaps less stable actin filaments are required for the dynamin-dependent fission of TGN-derived tubulo-vesicular carriers [16] compared with GAdTs containing components of different GA compartments.

Our observations also identified upstream regulators of LIMK1 and PKD1 involved in GOP formation. Previous studies have implicated RhoA in membrane trafficking and specifically in the regulation of endocytosis by recruiting Rock to rearrange the actin cytoskeleton [52]. While RhoA [15, 53] has been localized to the neuronal GA, its participation in shaping Golgi morphology and/or controlling transport has remained largely unexplored. We now extend these initial observations by showing not only that active RhoA is present in the neuronal GA, but that it also promotes GOP formation. Upon LPA stimulation active RhoA localizes to GAdTs restricted to the major dendrite; within deployed tubules, the highest RhoA activity was associated with spots positive for Golgi markers that resemble large GOPs. Together, these observations physically link active RhoA with the severing or fissioning of GAdTs and the local generation of large GOPs in dendrites. The possibility that RhoA regulates Golgi architecture by promoting fission or fragmentation is in line with a recent study in HeLa cells showing that expression of CA RhoA or CA mDia, a downstream target of Rho and a potent activator of actin polymerization, results in pronounced fragmentation of the GA into ministacks followed by dispersion into the cytoplasm [54]. In the case of neurons, LPA-induced RhoA activation did not result in fragmentation of the somatic GA. While the reason(s) underlying the differential response of the GA to RhoA activation between HeLa cells and neurons is not clear at present, one obvious possibility is a dosage-dependent effect [55] associated with activation of different downstream effectors (e.g., mDia versus Rock).

The RhoA-Rock-LIMK1/PKD1 signaling pathway appears not to be crucially required for tubule formation, elongation, or positioning. Thus, no alterations in the number of GAdTs were detected after inhibition of Rock with Y27632 or after suppression/inactivation of LIMK1 or PKD1; conversely, overexpression of LIMK1 or PKD1 did not increase the number of tubules entering the major dendrites or the proportion of dendrites displaying GAdTs. Thus, other factors may regulate tubule formation, positioning, and elongation during polarized GOP formation. One attractive possibility is the participation of Cdc42, another conspicuous member of the ras family of small RhoGTPases, with a crucial role in neuronal polarization [39], MTOC-GA positioning [56], and vesicle trafficking [56]. Cdc42 promotes dendritic development [39], and reelin promotes Cdc42- [23] or α-pix- [57] mediated GA deployment/translocation into the main dendrite. Interestingly, neurons from reelin-deficient mice have misorientation of apical dendrites; it has been proposed that, by favoring translocation of the GA, reelin may contribute to the selection of the process that becomes the apical dendrite [57]. It will now be of interest to evaluate the precise role of Cdc42 in GOP biogenesis, as well as the role of other GTPases (e.g., rabs), signaling pathways, and molecular motors. Finally, the generation of GOPs in minor dendrites still remains a mystery. In addition, the possibility exists that, once generated from GAdTs, maintenance of GOPs could be locally mediated by the dendritic ERES-ERGIC compartment. The recent development of novel pulse-chase procedures [58, 59] and the use of super-resolution microscopy [60] to follow ER to GA transport could provide a way to directly test the role of this compartment in the local generation of GOPs.

EXPERIMENTAL PROCEDURES

A detailed description of the techniques, materials, reagents, and constructs used in this study can be found in Supplemental Experimental Procedures.

SUPPLEMENTAL INFORMATION

Supplemental Information includes Supplemental Experimental Procedures and three figures and can be found with this article online at http://dx.doi.org/10.1016/j.cub.2015.01.075.

AUTHOR CONTRIBUTIONS

G.Q. and J.W. conducted all the experiments and data analysis. D.A.S. participated in live imaging experiments and also performed confocal microscopy. L.G. was responsible for generating cDNA constructs and participated in data analysis. M.P.M., C.C., M.B., and A. Couve participated in experimental design, data analysis, and discussion of results. In addition, M.B. and A. Couve carried out live-cell image experiments and participated in the writing of the manuscript. A. Cáceres supervised all steps of the research, including formulation of the working hypothesis, data analysis, and writing of the manuscript.

ACKNOWLEDGMENTS

This work was supported by grants from FONCyT (PICT V 2010-1277), CONICET, and Agencia Cordoba Ciencia to A. Cáceres and C.C. M.B. is supported by a return home grant from ISN. M.P.M. is supported by grants from FONDECyT. A. Couve and D.A.S. are supported by ICM P-09-015-F. G.Q. holds a doctoral fellowship from CONICET. M.B., C.C., and A. Cáceres are staff scientists from CONICET.

Received: June 20, 2014
Revised: December 2, 2014
Accepted: January 30, 2015
Published: March 19, 2015

REFERENCES

1. Torre, E.R., and Steward, O. (1996). Protein synthesis within dendrites: glycosylation of newly synthesized proteins in dendrites of hippocampal neurons in culture. J. Neurosci. *16*, 5967–5978.
2. Horton, A.C., and Ehlers, M.D. (2004). Secretory trafficking in neuronal dendrites. Nat. Cell Biol. *6*, 585–591.
3. Horton, A.C., Rácz, B., Monson, E.E., Lin, A.L., Weinberg, R.J., and Ehlers, M.D. (2005). Polarized secretory trafficking directs cargo for asymmetric dendrite growth and morphogenesis. Neuron *48*, 757–771.
4. Hanus, C., and Ehlers, M.D. (2008). Secretory outposts for the local processing of membrane cargo in neuronal dendrites. Traffic *9*, 1437–1445.
5. Ramírez, O.A., and Couve, A. (2011). The endoplasmic reticulum and protein trafficking in dendrites and axons. Trends Cell Biol. *21*, 219–227.
6. Jeyifous, O., Waites, C.L., Specht, C.G., Fujisawa, S., Schubert, M., Lin, E.I., Marshall, J., Aoki, C., de Silva, T., Montgomery, J.M., et al. (2009). SAP97 and CASK mediate sorting of NMDA receptors through a previously unknown secretory pathway. Nat. Neurosci. *12*, 1011–1019.
7. Ye, B., Zhang, Y., Song, W., Younger, S.H., Jan, L.Y., and Jan, Y.N. (2007). Growing dendrites and axons differ in their reliance on the secretory pathway. Cell *130*, 717–729.
8. Zheng, Y., Wildonger, J., Ye, B., Zhang, Y., Kita, A., Younger, S.H., Zimmerman, S., Jan, L.Y., and Jan, Y.N. (2008). Dynein is required for polarized dendritic transport and uniform microtubule orientation in axons. Nat. Cell Biol. *10*, 1172–1180.
9. Jan, Y.N., and Jan, L.Y. (2010). Branching out: mechanisms of dendritic arborization. Nat. Rev. Neurosci. *11*, 316–328.
10. Ori-Mc Kenney, K.M., Jan, L.Y., and Jan, Y.N. (2012). Golgi outposts shape dendritic morphology by functioning as sites of acentrosomal nucleation in neurons. Neuron *6*, 921–930.
11. Zhou, W., Chang, J., Wang, X., Savelieff, M.G., Zhao, Y., Ke, S., and Ye, B. (2014). GM130 is required for compartmental organization of dendritic golgi outposts. Curr. Biol. *24*, 1227–1233.
12. Nguyen, M.M., McCracken, C.J., Milner, E.S., Goetschius, D.J., Weiner, A.T., Long, M.K., Michael, N.L., Munro, S., and Rolls, M.M. (2014). Γ-tubulin controls neuronal microtubule polarity independently of Golgi outposts. Mol. Biol. Cell *25*, 2039–2050.
13. Cole, N.B., Sciaky, N., Marotta, A., Song, J., and Lippincott-Schwartz, J. (1996). Golgi dispersal during microtubule disruption: regeneration of Golgi stacks at peripheral endoplasmic reticulum exit sites. Mol. Biol. Cell *7*, 631–650.
14. Thayer, D.A., Jan, Y.N., and Jan, L.Y. (2013). Increased neuronal activity fragments the Golgi complex. Proc. Natl. Acad. Sci. USA *110*, 1482–1487.
15. Rosso, S., Bollati, F., Bisbal, M., Peretti, D., Sumi, T., Nakamura, T., Quiroga, S., Ferreira, A., and Cáceres, A. (2004). LIMK1 regulates Golgi dynamics, traffic of Golgi-derived vesicles, and process extension in primary cultured neurons. Mol. Biol. Cell *15*, 3433–3449.
16. Salvarezza, S.B., Deborde, S., Schreiner, R., Campagne, F., Kessels, M.M., Qualmann, B., Caceres, A., Kreitzer, G., and Rodriguez-Boulan, E. (2009). LIM kinase 1 and cofilin regulate actin filament population required for dynamin-dependent apical carrier fission from the trans-Golgi network. Mol. Biol. Cell *20*, 438–451.
17. Bisbal, M., Conde, C., Donoso, M., Bollati, F., Sesma, J., Quiroga, S., Díaz Añel, A., Malhotra, V., Marzolo, M.P., and Cáceres, A. (2008). Protein kinase d regulates trafficking of dendritic membrane proteins in developing neurons. J. Neurosci. *28*, 9297–9308.
18. Campelo, F., and Malhotra, V. (2012). Membrane fission: the biogenesis of transport carriers. Annu. Rev. Biochem. *81*, 407–427.
19. Kaech, S., Huang, C.F., and Banker, G. (2012). General considerations for live imaging of developing hippocampal neurons in culture. Cold Spring Harb. Protoc. *2012*, 312–318.
20. Maccioni, H.J., Quiroga, R., and Spessott, W. (2011). Organization of the synthesis of glycolipid oligosaccharides in the Golgi complex. FEBS Lett. *585*, 1691–1698.
21. Giraudo, C.G., Rosales Fritz, V.M., and Maccioni, H.J. (1999). GA2/GM2/GD2 synthase localizes to the trans-golgi network of CHO-K1 cells. Biochem. J. *342*, 633–640.
22. Giraudo, C.G., Daniotti, J.L., and Maccioni, H.J. (2001). Physical and functional association of glycolipid N-acetyl-galactosaminyl and galactosyl transferases in the Golgi apparatus. Proc. Natl. Acad. Sci. USA *98*, 1625–1630.
23. Matsuki, T., Matthews, R.T., Cooper, J.A., van der Brug, M.P., Cookson, M.R., Hardy, J.A., Olson, E.C., and Howell, B.W. (2010). Reelin and stk25 have opposing roles in neuronal polarization and dendritic Golgi deployment. Cell *143*, 826–836.
24. De Matteis, M.A., and Luini, A. (2008). Exiting the Golgi complex. Nat. Rev. Mol. Cell Biol. *9*, 273–284.
25. Bernard, O. (2007). Lim kinases, regulators of actin dynamics. Int. J. Biochem. Cell Biol. *39*, 1071–1076.
26. Sarmiere, P.D., and Bamburg, J.R. (2004). Regulation of the neuronal actin cytoskeleton by ADF/cofilin. J. Neurobiol. *58*, 103–117.
27. Bernstein, B.W., and Bamburg, J.R. (2010). ADF/cofilin: a functional node in cell biology. Trends Cell Biol. *20*, 187–195.
28. Lee-Hoeflich, S.T., Causing, C.G., Podkowa, M., Zhao, X., Wrana, J.L., and Attisano, L. (2004). Activation of LIMK1 by binding to the BMP receptor, BMPRII, regulates BMP-dependent dendritogenesis. EMBO J. *23*, 4792–4801.
29. Meng, Y., Zhang, Y., Tregoubov, V., Janus, C., Cruz, L., Jackson, M., Lu, W.Y., MacDonald, J.F., Wang, J.Y., Falls, D.L., and Jia, Z. (2002). Abnormal spine morphology and enhanced LTP in LIMK-1 knockout mice. Neuron *35*, 121–133.
30. Malhotra, V., and Campelo, F. (2011). PKD regulates membrane fission to generate TGN to cell surface transport carriers. Cold Spring Harb. Perspect. Biol. *3*, a005280, http://dx.doi.org/10.1101/cshperspect.a005280.
31. Yeaman, C., Ayala, M.I., Wright, J.R., Bard, F., Bossard, C., Ang, A., Maeda, Y., Seufferlein, T., Mellman, I., Nelson, W.J., and Malhotra, V. (2004). Protein kinase D regulates basolateral membrane protein exit from trans-Golgi network. Nat. Cell Biol. *6*, 106–112.
32. Curwin, A.J., von Blume, J., and Malhotra, V. (2012). Cofilin-mediated sorting and export of specific cargo from the Golgi apparatus in yeast. Mol. Biol. Cell *23*, 2327–2338.
33. von Blume, J., Duran, J.M., Forlanelli, E., Alleaume, A.M., Egorov, M., Polishchuk, R., Molina, H., and Malhotra, V. (2009). Actin remodeling by ADF/cofilin is required for cargo sorting at the trans-Golgi network. J. Cell Biol. *187*, 1055–1069.
34. von Blume, J., Alleaume, A.M., Cantero-Recasens, G., Curwin, A., Carreras-Sureda, A., Zimmermann, T., van Galen, J., Wakana, Y., Valverde, M.A., and Malhotra, V. (2011). ADF/cofilin regulates secretory cargo sorting at the TGN via the Ca2+ ATPase SPCA1. Dev. Cell *20*, 652–662.
35. Niwa, R., Nagata-Ohashi, K., Takeichi, M., Mizuno, K., and Uemura, T. (2002). Control of actin reorganization by Slingshot, a family of phosphatases that dephosphorylate ADF/cofilin. Cell *108*, 233–246.

36. Barišić, S., Nagel, A.C., Franz-Wachtel, M., Macek, B., Preiss, A., Link, G., Maier, D., and Hausser, A. (2011). Phosphorylation of Ser 402 impedes phosphatase activity of slingshot 1. EMBO Rep. *12*, 527–533.
37. Choi, J.W., Herr, D.R., Noguchi, K., Yung, Y.C., Lee, C.W., Mutoh, T., Lin, M.E., Teo, S.T., Park, K.E., Mosley, A.N., and Chun, J. (2010). LPA receptors: subtypes and biological actions. Annu. Rev. Pharmacol. Toxicol. *50*, 157–186.
38. Choi, J.W., and Chun, J. (2013). Lysophospholipids and their receptors in the central nervous system. Biochim. Biophys. Acta *1831*, 20–32.
39. Gonzalez-Billault, C., Muñoz-Llancao, P., Henriquez, D.R., Wojnacki, J., Conde, C., and Caceres, A. (2012). The role of small GTPases in neuronal morphogenesis and polarity. Cytoskeleton *69*, 464–485.
40. Pertz, O., Hodgson, L., Klemke, R.L., and Hahn, K.M. (2006). Spatiotemporal dynamics of RhoA activity in migrating cells. Nature *440*, 1069–1072.
41. Pertz, O. (2010). Spatio-temporal Rho GTPase signaling - where are we now? J. Cell Sci. *123*, 1841–1850.
42. Cowell, C.F., Yan, I.K., Eiseler, T., Leightner, A.C., Döppler, H., and Storz, P. (2009). Loss of cell-cell contacts induces NF-kappaB via RhoA-mediated activation of protein kinase D1. J. Cell. Biochem. *106*, 714–728.
43. Spratley, S.J., Bastea, L.I., Döppler, H., Mizuno, K., and Storz, P. (2011). Protein kinase D regulates cofilin activity through p21-activated kinase 4. J. Biol. Chem. *286*, 34254–34261.
44. Eisler, S.A., Fuchs, Y.F., Pfizenmaier, K., and Hausser, A. (2012). G-PKDrep-live, a genetically encoded FRET reporter to measure PKD activity at the trans-Golgi-network. Biotechnol. J. *7*, 148–154.
45. Tang, B.L. (2008). Emerging aspects of membrane traffic in neuronal dendrite growth. Biochim. Biophys. Acta *1783*, 169–176.
46. Hanus, C., Kochen, L., Tom Dieck, S., Racine, V., Sibarita, J.B., Schuman, E.M., and Ehlers, M.D. (2014). Synaptic control of secretory trafficking in dendrites. Cell Rep. *7*, 1771–1778.
47. Merianda, T.T., Lin, A.C., Lam, J.S., Vuppalanchi, D., Willis, D.E., Karin, N., Holt, C.E., and Twiss, J.L. (2009). A functional equivalent of endoplasmic reticulum and Golgi in axons for secretion of locally synthesized proteins. Mol. Cell. Neurosci. *40*, 128–142.
48. Aridor, M., and Fish, K.N. (2009). Selective targeting of ER exit sites supports axon development. Traffic *10*, 1669–1684.
49. González, C., and Couve, A. (2013). The axonal endoplasmic reticulum and protein trafficking: Cellular bootlegging south of the soma. Semin. Cell Dev. Biol. *27*, 23–31.
50. Sannerud, R., Marie, M., Nizak, C., Dale, H.A., Pernet-Gallay, K., Perez, F., Goud, B., and Saraste, J. (2006). Rab1 defines a novel pathway connecting the pre-Golgi intermediate compartment with the cell periphery. Mol. Biol. Cell *17*, 1514–1526.
51. Martínez-Alonso, E., Tomás, M., and Martínez-Menárguez, J.A. (2013). Golgi tubules: their structure, formation and role in intra-Golgi transport. Histochem. Cell Biol. *140*, 327–339.
52. Chi, X., Wang, S., Huang, Y., Stamnes, M., and Chen, J.-L. (2013). Roles of rho GTPases in intracellular transport and cellular transformation. Int. J. Mol. Sci. *14*, 7089–7108.
53. Camera, P., da Silva, J.S., Griffiths, G., Giuffrida, M.G., Ferrara, L., Schubert, V., Imarisio, S., Silengo, L., Dotti, C.G., and Di Cunto, F. (2003). Citron-N is a neuronal Rho-associated protein involved in Golgi organization through actin cytoskeleton regulation. Nat. Cell Biol. *5*, 1071–1078.
54. Zilberman, Y., Alieva, N.O., Miserey-Lenkei, S., Lichtenstein, A., Kam, Z., Sabanay, H., and Bershadsky, A. (2011). Involvement of the Rho-mDia1 pathway in the regulation of Golgi complex architecture and dynamics. Mol. Biol. Cell *22*, 2900–2911.
55. Ng, J., and Luo, L. (2004). Rho GTPases regulate axon growth through convergent and divergent signaling pathways. Neuron *44*, 779–793.
56. Harris, K.P., and Tepass, U. (2010). Cdc42 and vesicle trafficking in polarized cells. Traffic *11*, 1272–1279.
57. Meseke, M., Rosenberger, G., and Förster, E. (2013). Reelin and the Cdc42/Rac1 guanine nucleotide exchange factor αPIX/Arhgef6 promote dendritic Golgi translocation in hippocampal neurons. Eur. J. Neurosci. *37*, 1404–1412.
58. Al-Bassam, S., Xu, M., Wandless, T.J., and Arnold, D.B. (2012). Differential trafficking of transport vesicles contributes to the localization of dendritic proteins. Cell Rep. *2*, 89–100.
59. Boncompain, G., and Perez, F. (2013). Fluorescence-based analysis of trafficking in mammalian cells. Methods Cell Biol. *118*, 179–194.
60. Pellett, P.A., Dietrich, F., Bewersdorf, J., Rothman, J.E., and Lavieu, G. (2013). Inter-Golgi transport mediated by COPI-containing vesicles carrying small cargoes. eLife *2*, e01296.

